REVIEW

Osteoarthritis and magnetic resonance imaging: potential and problems

C W Hutton, W Vennart

Magnetic resonance imaging (MRI) is in its infancy. Despite widespread clinical applications it has enormous unrealised potential. Unlike all other imaging modalities, it is intrinsically a varied technology that has to be engineered for each problem investigated. Present imaging using whole body systems lacks specificity and resolution, but this should eventually be overcome using tailor made dedicated equipment such as specialised surface coils and targeted gradient coils. MRI offers potential for in vivo non-invasive measurement and imaging that may revolutionise the understanding of osteoarthritis (OA). Currently, there are no known physiological hazards associated with the magnetic field and gradient strengths used in routine MRI systems, and there is no other non-invasive method that allows repeat imaging of specific aspects of the joint without the use of ionising radiation and hence promises insight into the interactions between the different structures or the processes that are involved in joint physiology and pathology. Understanding the potential of MRI to investigate OA requires an insight into the physics of the technique.

Basic physics of MRI

Nuclear magnetic resonance (NMR) was developed as a method for studying the atomic nucleus and chemical composition of materials.[1][2] With the development of methods of localising nuclear signals, it was extended to imaging.[3] MRI is primarily concerned with mapping the distribution of protons within hydrogen atoms.[4] When protons, which spin on their axes and possess a magnetic moment, are immersed in a homogeneous magnetic field (B_o) they precess around the field with orientations allowed by quantum mechanics that are parallel and anti-parallel to the field corresponding to low and high energy states. The frequency of the precession is given by $\omega_o = \gamma B_o$, where γ is the ratio of the magnetic moment of the nucleus to its angular momentum. The majority of commercial imaging systems operate in the range of values of $B_o = 0 \cdot 5 - 1 \cdot 5$ Tesla (T), the corresponding proton precessional frequencies being 20–60 MHz.

If the protons are exposed to a pulse of radiofrequency radiation in a plane perpendicular to B_o, they are displaced from equilibrium and precess around B_o in the plane of the radiofrequency radiation. After the radiofrequency pulse is switched off, the

protons return to equilibrium with a process that involves the dephasing of the spinning protons relative to each other, and one that restores the equilibrium of low and high energy states. The former process, spin-spin relaxation, is determined by a constant, T2; the latter, spin-lattice relaxation, by a constant, T1. Both T1 and T2 vary and depend on a set of parameters such as tissue composition, field strength, and temperature. As the spinning protons relax back to equilibrium, their associated magnetisations vary in time and space. This can induce a current in a coil of wire wound round the sample. To derive data for MRI experiments, this signal is amplified and its amplitude, frequency and phase measured. Figure 1 illustrates this process.

The proton precessional frequency (the Larmor equation) is influenced by different chemical environments which produce a shielding effect on the proton, such that the Larmor equation becomes $\omega = \gamma B_o (1 - \delta)$; B_o is the applied field and δ is a shielding factor. The shielding factor gives information about the chemical composition of the material and is the basis of magnetic resonance spectroscopy.

The position of the protons giving rise to the MRI signal can be identified by applying magnetic field gradients across the sample. The gradient causes the resonant frequency to vary with spatial position according to the

Mount Gould Hospital, Plymouth, United Kingdom
C W Hutton

Department of Physics, University of Exeter, Exeter, United Kingdom
W Vennart
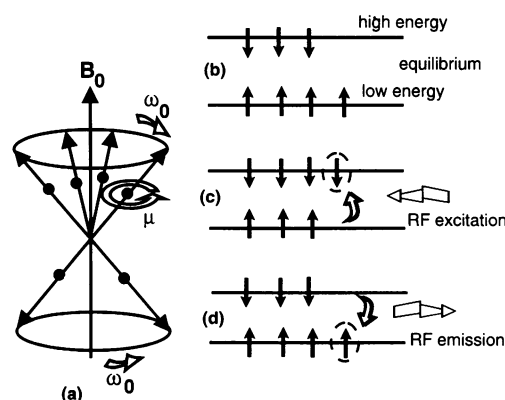
Figure 1   (a) Water protons spinning and precessing in equilibrium in a static magnetic field B_o; protons are quantum particles—just a few more than half will precess with the field (low energy state) and slightly less against the field (high energy state). (b) This equilibrium distribution can be represented diagramatically as two energy levels with more protons in the lower level (↑) than the upper level (↓). (c) Application of a burst of radiofrequency (RF) radiation to the system excites a net number of protons from the low to the high energy state. (d) When the RF is removed the spins return to equilibrium by emitting RF radiation—this is detected in the MRI investigation.

equation $\omega = \gamma \ (B_o + rG_r) \ (1 - \delta)$, where r is spatial position and G_r the magnetic field gradient $[(dB_o)/dr]$ in the direction r. In most cases, δ is only a small correction factor and the equation can be written $\omega = \gamma \ (B_o + rG_r)$; in this way ω (frequency) is proportional to r (position) for constant B_o and G_r. Applying magnetic field gradients to an object, the frequency of precession of the protons is proportional to position (fig 2). By appropriate manipulation of gradients in three orthogonal directions during excitation of the protons, and collecting signals obtained from a sample when the protons relax back to equilibrium, an image of spatial variation of the proton density can be produced.

The images are generated by Fourier transformation of the time varying data giving the frequency distribution of the protons in an object. Images are generated with 64×64, 128×128, 256×256 or 512×512 pixels (or variations of these), with varying section thickness according to the resolution required. The signal in each pixel is a function of B_o, T1, T2, and proton density.

The imaging experiment takes time. In particular, it is limited by acquisition of phase encoding data. During this time there is a problem with movement altering spatial relationships, for example movement from the patient, and flow of protons in tissues by such activities as perfusion and diffusion; resonant protons will move within or out of the selected slice. This problem of movement can be turned to advantage to give information on flow and perfusion or diffusion.

Pulse sequences

The MRI experiment is usually designed to generate signal and signal contrast between tissues at adequate resolution. This is achieved by selecting appropriate radiofrequency and magnetic field gradient pulse sequences, field strength, pixel size, and slice thickness. There are a bewildering variety of pulse sequences used to generate images. The common pulse sequence used is spin-echo. This sequence rephases protons dephased by magnetic field inhomogeneities and thereby increases signal. However this rephasing takes time and thus the experiment takes too long to capture enough signal from tissues with very short T2, such as hyaline cartilage; this is better achieved with gradient-echo pulse sequences. However the gradient-echo image is potentially distorted by the magnetic susceptibility differences of tissues in high magnetic fields. Optimum tissue discrimination particularly between effusion, cartilage and soft tissue has been explored with modifications of these pulse sequences.[5]

Flow and diffusion imaging

The MRI experiment can yield flow information in two ways: first, by measuring signal in an adjacent slice to give a time of flight angiograph;[6] and second, by measuring changes in phase of the MRI signal during the application of a field gradient. If two oppositely directed gradient pulses are applied, all protons that have not moved will have their phase induced by the first exactly cancelled by the second pulse. If a proton has moved, this will be incomplete, and a net phase shift proportional to velocity can be observed. When information is obtained in all three planes patterns of flow can be built up; again, motion will distort the images obtained.[7]

A similar phase change method gives information about non-directional movement (primarily, diffusion). Longer duration phase encoding gradients are needed, as the distances are smaller. If the voxel (three dimensional pixel) is large, this apparently random movement will include capillary flow; it measures the incoherent displacement, as opposed to the coherent displacement of flow and thus is termed intravoxel incoherent motion.[8] Enhanced information on flow can be produced by using contrast agents that alter the relaxation characteristics of the moving fluid.

Figure 2 (a) The application of a magnetic field gradient to two tubes of water in a magnetic field B_o at positions r_1 and r_2 endows the protons within them with different Larmor frequencies, ω_1 and ω_2. (b) The time varying signals received from each sample after excitation with a burst of radiofrequency (RF) radiation will have different rates of variation because the RF radiation emitted is determined by the magnetic field strength. (c) The combined signals will superimpose and give a more complicated time varying pattern which can be analysed using a Fourier transform. (d) In this case two frequencies, ω_1 and ω_2, will be present and since field strength (and Larmor frequency) is proportional to position, ω_1 and ω_2 can be directly related to the positions of the tubes of water r_1 and r_2.

Biochemistry

The chemical shift effect produced by the local molecular environment of protons causing changes in the magnetic field they experience allows information about the tissue composition to be derived. The abundance of protons in organic molecules means that the proton is the most attractive atomic nucleus to measure. Other atoms with intrinsic spin, such

as phosphorous-31 and sodium-23, can also be used.[9] Similarly, the non-radioactive carbon-13 can be used as a tracer compound for in vivo experiments. The concentration of these nuclei is approximately 1000 times less than that of water and thus the signal is much reduced. At present this means that volumes of approximately 15 ml are needed for in vivo phosphorous spectroscopy, but as techniques improve this may be reduced to a more physiologically appropriate size, particularly for in vitro analysis.

Tissue hydration

Water is an ideal molecule to study with MRI. In OA, hydration changes in the cartilage are striking. Both experimentally and in analysis of OA samples, there appears to be an initial increase in water and then, in severe disease, a loss. This should be reflected in changes in the T2 and T1 of the tissue,[10] and consequently, measuring tissue T1 and T2 provides information on the organisation of their water content.[11]

In OA, T1 changes in cartilage have been explored in vitro and related to water content and histological scale of severity.[12] It was found that T1 values for cartilage less than 2·5 s (measured at 9·6 T—this was an experimental system, not a clinical one) appeared to be associated with early OA, but greater values may also relate to early stages of the disease process, when a higher percentage of free water is present. Improvements to imaging techniques are being made and in vitro studies of bovine cartilage have shown differences in water concentrations between superficial and deep layers.[13]

High resolution

To image a tissue in which changes are focal and at microscopic level requires high resolution MRI. Images of tissue down to 100 μm can be achieved[14-16] using magnetic field strengths of 0·5–4·7 T; higher resolution imaging is being considered, but movement of subjects is difficult to control below this level. For further improvements, the problems of water diffusion and blood perfusion will have to be addressed, as these degrade images. The major problem however, is that MRI has a poor signal to noise ratio; it is intrinsically an inefficient system. Noise derives from the imaging system and from the subject. The former source includes problems with hardware, such as stability of the magnetic field gradients, and the development of eddy currents in superconducting magnet system, while the latter includes motion artefact. Signal can be improved by increasing field strength and by improving signal acquisition with specifically designed surface coils; however, as field strength is increased, artefacts caused by susceptibility changes in tissues are more pronounced, and thus image interpretation must be undertaken with care.[15] Much of the body, including deep and large joints, is too remote to allow high resolution imaging.

Joint movement

Joints are intrinsically dynamic structures, and their failure in OA must relate to movement. The static frame of most imaging systems means that this tends to be ignored. The knee is seen and studied in extension, and serial images can be built up from conventional images to give a dynamic picture. Faster imaging by ultrafast spoiled GRASS imaging[17 18] and echo planar imaging make real time imaging possible, but again there is a problem with low signal for high resolution.[19] This technique has allowed variation in patella tracking to be identified, and showed the importance of failure of normal tracking in the earliest phase of flexion.

MRI imaging of joint structures

CARTILAGE

Cartilage should be an ideal tissue for proton MRI imaging. It is largely water, held by the hydrostatic attraction of proteoglycan molecules trapped by a network of collagen.[20] The proteoglycans form a gel, with water bound to the molecules and hydration shells developing around the bound layer.[21] The effect of the organisation of water in relation to macromolecules has been demonstrated with type II collagen.[22 23] Water away from the hydration sphere is essentially 'free', while that close to macromolecules is bound. The spin-spin relaxation time of these water protons is heavily dependent on the relatively static environment of the macromolecules—this produces short T2 values. T2 and T1 measurements of dextran and polyacrylamide gels are sensitive to pore size, with a critical size, G25, at which the relaxation times increased.[24]

BONE

The imaging of bone poses a problem. The calcified matrix has a T2 that is short, thus at present signal is impossible to capture and is imaged as a signal void. The signal void varies with the thickness of the bone and should reflect the subchondral sclerosis of OA. Bone marrow produces a signal; the pattern may provide information on the organisation of bone. In OA, the marrow becomes hyperaemic with venous congestion; these changes should be detectable as changes in hydration, flow, or diffusion.

The specific problems of imaging bone are partial volume effects, susceptibility, and chemical shift of bone marrow fat signals. As noted previously, the chemical shift is a function of the chemical environment of protons; those associated with water have a Larmor frequency shift of 3·5 ppm compared with those associated with fat. As localisation is dependent on the phase and frequency of the MRI signal, positional data will differ for the two types of tissue in the same position: one associated with water, the other with fat. The difference will increase with increasing magnetic field strength; at low resolution this may be a small shift for large structures, but with increased magnification the effect
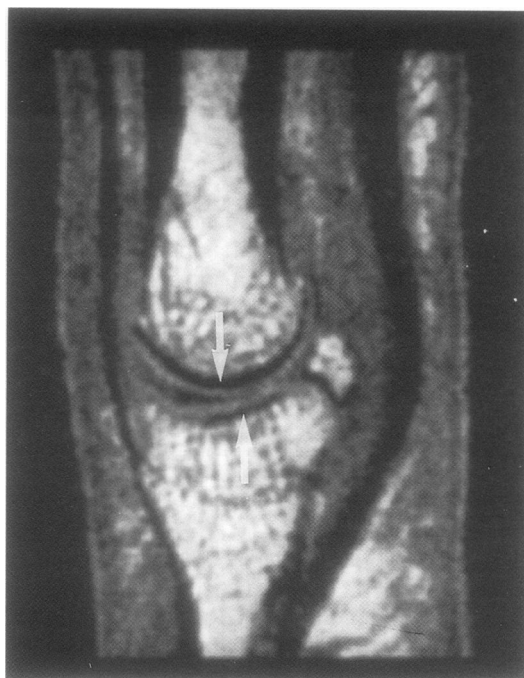
Figure 3   Part of a three dimensional set of images through the thumb joint of a normal volunteer taken with a gradient-echo sequence with TE = 6 ms and TR = 200 ms. The arrows indicate the different thickness of signal void generated by subchondral bone and the chemical shift of bone marrow fat signal into this area. Reversal of the magnetic field gradient would reverse this asymmetry of the signal void around the bone ends.

becomes a significant distortion. The direction of the shift is dependent on the magnetic field gradient direction, and thus will alter with the orientation of the tissue in the magnetic field. In figure 3 subchondral bone images as a void; this is larger on one side of the joint compared with the other—an asymmetry that reverses with reversal of the field gradient. Distortions also occur from the marrow signal moving into the true trabecular bone structure. A number of methods have been proposed to try to remove the distortion by imaging fat and water separately.[25-28]

Most images of the marrow fail to resolve the boney microstructure and each voxel will be a varying mix of the signal from water, fat, and the void generated by bone. Quantitative chemical shift imaging shows promise in demonstrating overall effects in the marrow, but better resolution is needed to identify the component structures.[29] The proportion of fat, red haematopoietic marrow and bone vary with age; it has also been found that the effective T1 and T2 vary with age.[30]

Bone is a diamagnetic material that will alter the local value of the magnetic field strength when immersed in a static field B_o.[31] This has two effects: loss of signal because of reduction of T2, and geometric distortions.[32] Experimentally, this can be demonstrated as a change in T2 when water is mixed with powdered bone—there is little alteration in T1.[33] Spin-echo sequences rephase static imhomogeneities in the magnetic field, and thus reduce this effect. The change in T2 may be used to give information on changes in the bone content and structure of trabeculae;[34] it may also explain changes in bone marrow signal

between the end and middle of long bone where there is relatively more trabecular bone.[35]

TENDON AND SOFT TISSUES

Tendon also has a short T2 and is imaged as a signal void. Contrast around tendons increases with increase in signal from the sheaths, relative to the tendon signal void, but if the fibrous tissue gives a signal the contrast is reduced and structures such as the triangular ligament of the wrist will be lost as they become isointense with the surrounding tissue.[36] As structures move, the effect of structural orientation within the field may produce distortion of the image. Orientation is important in determining effects such as chemical shift and susceptibility, as observed in the change of shape and signal of tendons with orientation.[37] It has been suggested that the orientation of the collagen fibrils gives the tissue a structural anisotropy which changes T2 with tendon orientation.[38]

MRI in osteoarthritis

The use of routine clinical MRI machines (0·5–2·0 T) in investigating OA has been limited and primarily concerned with the identification of anatomical changes—it has allowed access to deep axial joints.[39]

Most studies in man have been preliminary assessments and have studied the knee. Changes in soft tissue, particularly in the menisci, have been identified. Spin-echo sequences show fibrocartilage as signal void, but changes in the meniscus, allowing an increase in free water, give increased signal contrast; this may be associated with a tear or mucinoid degeneration.[40] MRI studies which show the ligaments and relationships between cruciate instability, meniscal lesions, cartilage thinning, and bone change are now being reported.[41] In OA, meniscal changes seem to be common, with abnormal and varied signals also being seen, relating to subchondral cysts and osteophytes.[42] It is not clear how well arthroscopy correlates with these MRI features of OA.[43] In post-traumatic OA, MRI may reveal an occult fracture.[44] Figure 4 shows a typical MR image of a knee joint in a patient with osteoarthritis.

In the hip, spheroidal cartilage cuts the imaging plane. This increases the risk of partial volume effects, which throws into question the accuracy of the small number of studies completed which explore the value of MRI in grading hip disease.[45] Using gradient-echo fast imaging steady state procession (FISP) sequences, thinning of the cartilage and focal intensity changes could be detected in elderly volunteers, suggesting that it might be possible to detect early presymptomatic change.[46] However, more formal studies of cartilage have demonstrated a lack of precision when using MRI for quantitative measurements.[47-49]

Interpretation of the MRI changes is difficult. Initial studies comparing MRI with other imaging modalities demonstrated the
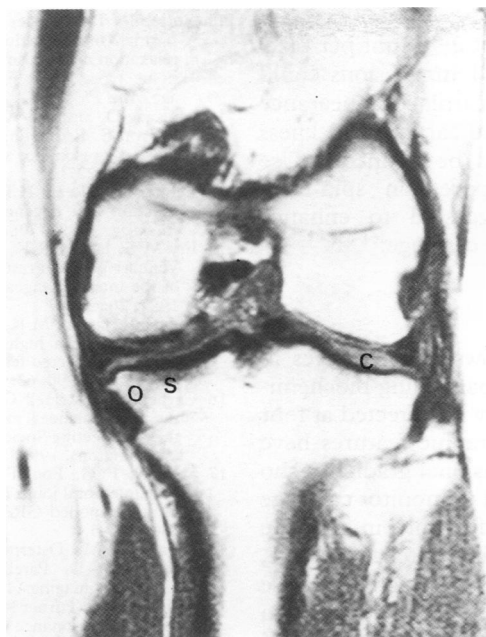
Figure 4   Spin-echo images of an osteoarthritic knee. The sequence used had a TR of 500 ms and TE of 25 ms and slice thickness of 4 mm. The image illustrates: cartilage (C) as grey but partial volume effects and lack of contrast with synovial fluid makes the edges unclear; an area of decreased marrow signal in subchondral bone sclerosis (S); and (O) osteophyte formation.

variation in MRI features and difficulty in understanding change in relation to techniques that focus primarily on bone change.[50] MRI, however, also allows study of changes early in the evolution of disease, demonstrating in vivo changes that could previously only be inferred from pathological study.[51] The process of interpretation is restricted by poor resolution and tissue discrimination; improved higher resolution imaging should overcome this and show early changes in joint and periarticular structures, for example a growing Heberden's node (fig 5). A similar variation and problem of interpretation has been found with analysis of osteoarthritic synovial fluid.[52] In the temporomandibular joint, MR has suggested much more frequent degenerative change which may be the basis of facial skeleton remodelling.[53]

Cartilage in other diseases

Experience in other bone and cartilage disorders suggests considerable information may be derived from conventional MR scanning used in routine clinical practice. In Perthe's disease of the hip, an increase in cartilage thickness has been identified,[54] in addition to early cartilage fractures after avascular necrosis.[55] Chondromalacia shows changes similar to fibrillation and cartilage cratering, but at low resolution confidence in defining early change has been poor.[56-59] In allogenic cartilage transplants, spin-echo imaging shows bone, but gradient-echo sequences illustrated cartilage degeneration and oedema;[60] in trauma, subchondral bone bruising, undetected cruciate tears, and subchondral fracture are identified by MRI, suggesting greater sequelae than has previously been appreciated.[61]

The accuracy of resolving defects in cartilage has been addressed by several workers, with conflicting reports concerning identification of cartilage thinning, craters, and fibrillation. Gadolinium contrast medium is needed to identify small full thickness 2 mm lesions on T1 weighted images, but even 5 mm lesions were occult on T1 weighted images without gadolinium.[62] Other studies of 3 mm slice
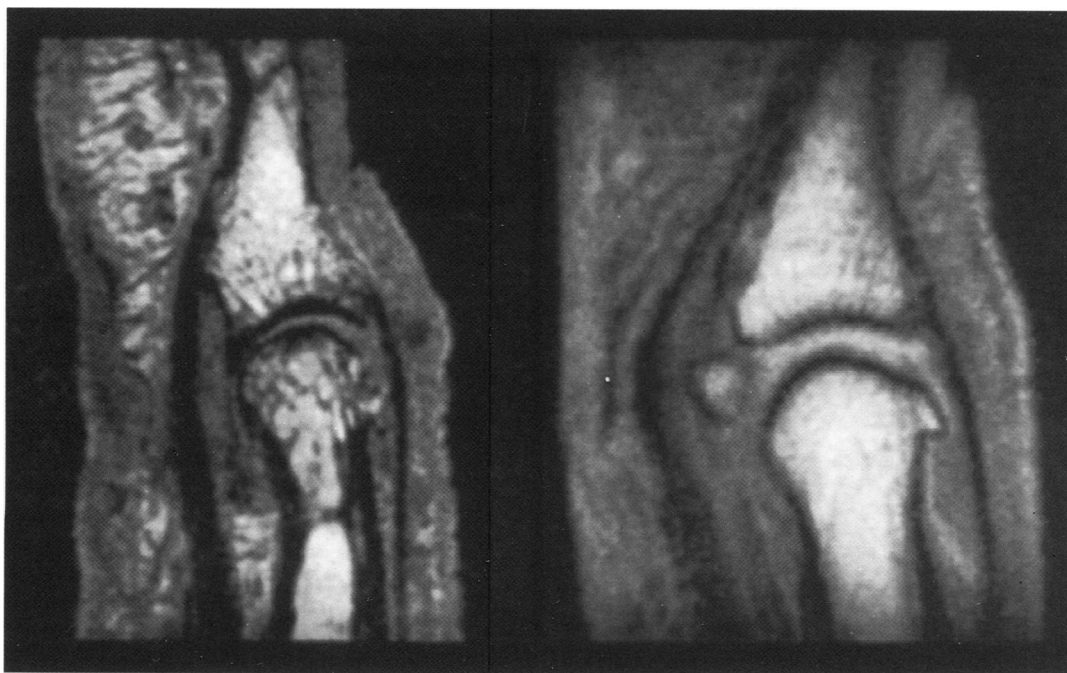
Figure 5   Left: Part of multi-slice two dimensional set of images through the thumb joint of a patient suffering from osteoarthritis, using a gradient-echo sequence—the osteophyte formation was not revealed by x radiography. Right: Part of three dimensional set of images of the distal interphalangeal joint of a patient suffering from osteoarthritis, showing unequal distribution of cartilage thinning.

thickness spin-echo images (TR 600ms, TE 17ms) with a resolution of 0·95 mm per pixel and B₀ of 1 T suggested 1 mm lesions could be identified. The gross cartilage appearance was well demonstrated and cartilage thickness variation of 1 mm could be defined.[63] Use of T1 weighted fat suppression spin-echo sequences has been suggested to enhance lesion detection in hyaline cartilage.[64][65]

Experimental OA

Anterior cruciate OA shows MRI changes in cartilage with thickening paralleling biochemical activity.[66] Changes may be detected at four weeks, before any radiographic features have developed.[67] Three dimensional gradient-echo imaging[68][69] has been used to monitor cartilage change; this was successful only in the late stages of disease. In bovine patella cartilage, use of both T1 and T2 weighted pulse sequences permitted detection of two layers in cartilage, correlating with the tangential and transitional zones. Differential effects on the signal with pressure and in early degenerative change have suggested that there was increased hydration in the superficial layer.[70] Injection of papain into a joint to induce OA produces a loss of signal and a narrowing of the cartilage, which can be partly resolved.[71] Quantitative MRI has been used in the study of rhesus macaques[72] and the analysis of the evolution of OA of the guinea pig.[73]

Summary

To date, MRI has primarily been used to study anatomical changes, and at a resolution that makes detailed analysis of focal change difficult. This is primarily because cost limits the development and use of tailor made research systems. The detailed analysis of soft tissue, cartilage, and bone marrow images should provide a fruitful non-invasive method to study OA. However, the development of MRI methods to study movement, diffusion and perfusion, and the spatial localisation of spectroscopic information, promises a revolution in the study of the living joint in man.

1 Bloch F, Hanson W, Packard M E. Nuclear induction. *Physical Review* 1946; **69:** 127.
2 Purcell E M, Torrey H C, Pound R V. Resonance absorption by nuclear magnetic moments in a solid. *Physical Review* 1946; **69:** 37–8.
3 Lauterbaur P C. Image formation by induced local interactions; examples employing nuclear magnetic resonance. *Nature* 1973; **242:** 190–1.
4 Moonsen C T W, van Zijl P C M, Frank J A, Le Bihan D, Becker E D. Functional magnetic resonance imaging in medicine and physiology. *Science* 1990; **250:** 53–60.
5 Konig H, Sauter R, Deimling M, Vogt M. Cartilage disorders: comparison of spin echo, CHESS and FLASH sequence MRI images. *Radiology* 1988; **164:** 753–8.
6 Axel L. Blood flow effects in magnetic resonance imaging. *Am J Roentgenol* 1984; **143:** 1157–66.
7 Hennig J, Muri M, Brunner P, Friedburg H. Quantitative flow measurement with the fast flow fourier technique. *Radiology* 1988; **166:** 237–40.
8 Le Bihan D, Breton E, Lallemand D, Aubin M L, Vignaud J, Laval-Jeantet M. Separation of diffusion and perfusion in intravoxel incoherent motion MRI imaging. *Radiology* 1988; **168:** 497–505.
9 Hoult D I. Observations of tissue metabolism using 31P nuclear magnetic resonance. *Nature* 1974; **252:** 285–7.
10 Mathur-De Vre R. Biomedical implications of the relaxation behaviour of water related to NMR imaging. *Br J Radiol* 1984; **57:** 955–76.

11 Bottomley P A, Foster T H, Argersinger R E. A review of normal tissue hydrogen NMR relaxation time and relaxation mechanisms from 1–100 MHz: dependence on tissue type, NMR frequency, temperature, species and age. *Med Phys* 1984; **11:** 425–48.
12 McKeag D, Smith B W H, Edminster R, Laird T, Clark J, Herron S. Estimating the severity of osteoarthritis with magnetic resonance spectroscopy. *Semin Arthritis Rheum* 1992; **21:** 227–38.
13 Lehner K B, Rechl H P, Gmeinwieser J K *et al.* Structure, function and degeneration of bovine hyaline cartilage. *Radiology* 1989; **170:** 495–9.
14 Fry M E, Jacoby R K, Hutton C W, Ellis R E, Pittard S, Vennart W. High resolution magnetic resonance imaging of the interphalangeal joints of the hand. *Skeletal Radiol* 1991; **20:** 273–7.
15 Cole P R, Jassani M K, Wood B, Freemont J, Morris G A. High resolution, high field magnetic resonance imaging of joints: unexpected features in proton images of cartilage. *Br J Radiol* 1990; **63:** 907–9.
16 Carpenter T A, Hall C D, Hodgson R J. Investigation of the interphalangeal joint under flexion. In: Proceedings of the 8th Meeting Society for Magnetic Resonance Imaging (Washington), 1990; 262.
17 Shellock F G, Foo T K F, Deutsch A L, Mink J H. Patellofemoral joint: evaluation during active flexion with ultrafast spoiled GRASS MRI imaging. *Radiology* 1991; **180:** 581–5.
18 Kujala U M, Osterman K, Kormano M, Komu M, Schlenzka D. Patella motion analysed by magnetic resonance imaging. *Acta Orthop Scand* 1989; **60:** 13–6.
19 Stehling M K, Turner R, Mansfield P. Echo planar imaging: magnetic resonance imaging in fraction of a second. *Science* 1991; **254:** 43–50.
20 Caplan A I. Cartilage. *Sci Am* 1984; **251:** 84–94.
21 Kuntz I D Jr, Brassfield T S, Law G D, Purcell G V. Hydration of macromolecules. *Science* 1969; **163:** 1329–31.
22 Berendsen H J C. Nuclear magnetic resonance study of collagen hydration. *J Chem Phys* 1962; **36:** 3297–305.
23 Kim D K, Ceckler T L, Mascall V C, Calabro A, Balabon R S. Analysis of water-macromolecule proton magnetization transfer in articular cartilage. *Magn Reson Med* 1993; **29:** 211–5.
24 Murase N, Watanabe T. Nuclear magnetic relaxation studies of the compartmentalized water in crosslinked polymer gels. *Magn Reson Med* 1989; **9:** 1–7.
25 Chan T W, Listerud J, Kressel H Y. Combined chemical shift and phase selective imaging for fat suppression: theory and initial clinical experience. *Radiology* 1991; **181:** 41–7.
26 Keller P J, Hunter W W Jr, Schmalbrock P. Multisection fat water imaging with chemical shift selective presaturation. *Radiology* 1987; **164:** 539–41.
27 Dixon W T. Simple proton spectroscopic imaging. *Radiology* 1984; **153:** 189–94.
28 Williams S C R, Horsfield M A, Hall L D. True water and fat MRI imaging with use of multiple echo acquisition. *Radiology* 1989; **173:** 249–53.
29 Rosen B R, Fleming D M, Kushner D C, *et al.* Haematologic bone marrow disorders: quantitative chemical shift MRI imaging. *Radiology* 1988; **169:** 799–804.
30 Vogler J B, Murphy W A. Bone marrow imaging. *Radiology* 1988; **168:** 679–93.
31 Majumdar S, Gore J C. Studies of diffusion in random fields produced by variations in susceptibility. *J Magn Reson* 1988; **78:** 41–55.
32 Rosenthal H, Thulborn K R, Rosenthal B R, Kim S H, Rosen B R. Magnetic susceptibility effects of trabecular bone on magnetic resonance imaging of bone marrow. *Invest Radiol* 1990; **25:** 173–8.
33 Davis C A, Genant H K, Dunham J S. The effects of bone on proton NMR relaxation times of surrounding liquids. *Invest Radiol* 1986; **21:** 472–7.
34 Wehrli F W, Ford J C, Attie M, Kressle H Y, Kaplan F S. Trabeculae structure: preliminary application of MRI interferometry. *Radiology* 1991; **179:** 615–21.
35 Sebag G H, Moore S G. Effect of trabecular bone on the appearance of marrow in gradient echo imaging of the appendicular skeleton. *Radiology* 1990; **174:** 855–9.
36 Wong E C, Jesmanowicz A, Hyde J S. High resolution imaging of the fingers and wrist with a local gradient coil. *Radiology* 1991; **181:** 393–7.
37 Erickson S J, Cox I H, Hyde J S, Carrera G F, Strandt J A, Estkowski R T R. Effect of tendon orientation on MRI imaging signal intensity: a manifestation of the magic angle phenomenon. *Radiology* 1991; **181:** 389–92.
38 Fullerton G D, Cameron I L, Ord V A. Orientation of tendons in the magnetic field and its effect on T₂ relaxation times. *Radiology* 1985; **155:** 433–5.
39 Grenier N, Kressel H Y, Schiebler M L, Grossman R I, Dalinka M K. Normal and generative posterior spinal structures: MRI imaging. *Radiology* 1987; **165:** 517–25.
40 Stroller D W, Martin C, Crues J V, Kaplan L, Mink J H. Meniscal tears: pathologic correlation with MRI imaging. *Radiology* 1987; **163:** 731–5.
41 Spritzer C E, Vogler J B, Martinez S, *et al.* MRI imaging of the knee; preliminary results with a 3D GRASS pulse sequence. *Am J Roentgenol* 1988; **150:** 597–603.
42 McAlindon T E M, Watt I, McCrae F, Goddard P, Dieppe P A. Magnetic resonance imaging in osteoarthritis of the knee: correlation with radiographic and scintigraphic findings. *Ann Rheum Dis* 1991; **50:** 14–9.

43 Adams M E, Li D K, McConkey J P, *et al.* Evaluation of cartilage lesions by magnetic resonance imaging at 0.15T: comparison with anatomy and concordance with arthroscopy. *J Rheum* 1991; 18: 1573–80.

44 Vellet A D. The evolutions of post-traumatic osteoarthritis: its relationship to occult post-traumatic subcortical fractures identified on MRI. *Bildgebung* 1992; 59: 121–2.

45 Li K C, Higgs J, Aisen A M, Buckwalter K A, Martel W, McCune W J. Magnetic resonance imaging in osteoarthritis of the hip: gradations of severity. *Magn Reson Imaging* 1988; 6: 229–36.

46 Bongartz G, Bock E, Horbach T, Requardt H. Degenerative cartilage lesions of the hip—magnetic resonance evaluation. *Magn Reson Imaging* 1989; 7: 179–86.

47 Jonsson K, Buckwalter K, Helvie M, Niklason L, Martel W. Precision of hyaline cartilage thickness measurements. *Acta Radiologica* 19922; 33: 234–9.

48 Recht M P, Kramer J, Marcelis S, *et al.* MR assessment of abnormalities of articular cartilage in the knee: an analysis of available techniques. *Radiology* 1993; 187: 473–8.

49 Hodler J, Trudell D, Pathria M N, *et al.* Width of the articular cartilage of the hip: quantification by using fat suppression spin echo MR imaging in cadavers. *Am J Roentgenol* 1992; 195: 351–5.

50 Chan W P, Lang P, Stevens M P, *et al.* Osteoarthritis of the knee: comparison of radiology, CT and MRI imaging to assess extent and severity. *Am J Roentgenol* 1991; 157: 799–80.

51 Fernandez-Madrid F, Karvonen R L, Teitge R A, Reed A H, Ndgendank W G. Early features of osteoarthritis of the knee studied by MRI imaging. *Proc Soc Magn Reson Med* 1991; 63.

52 Williamson M P, Humm G, Crisp A J. H-1 nuclear magnetic resonance investigation of synovial fluid component in osteoarthritis, rheumatoid arthritis and traumatic effusions. *Br J Rheumatol* 1989; 28: 23–7.

53 Schellhas K P, Piper M A, Omlie M R. Facial skeleton remodeling due to temporomandibular joint degeneration: an imaging study of 100 patients. *Am J Neuroradiol* 1990; 11: 541–51.

54 Rush B H, Bramson R T, Ogden J A. Legg Calve Perthe's Disease: detection of cartilagenous and synovial changes with MRI imaging. *Radiology* 1988; 167: 473–6.

55 Schuman W P, Castagno A A, Baron R L, Richardson M L. MRI imaging of avascular necrosis of the femoral head: value of small field of view sagittal surface coil images. *Am J Roentgenol* 1988; 150: 1073–8.

56 Reiser M F, Bongartz G, Erlemann R, *et al.* Magnetic resonance in cartilagenous lesions of the knee joint with three dimensional gradient echo imaging. *Skel Radiol* 1988; 17: 465–71.

57 Yulish B S, Montanez J, Goodfellow D B, Bryan P J, Mulopulos G P, Modic M T. Chondromalacia patellae: assessment with MRI imaging. *Radiology* 1987; 164: 763–6.

58 Hayes C W, Sawyer R W, Conway W F. Patella cartilage lesions; in vitro detection and staging with MRI imaging and pathologic correlation. *Radiology* 1990; 176: 479–83.

59 McCauley T R, Kier R, Lynch K J, *et al.* Chondromalacia patella. Diagnosis with MR imaging. *Am J Roentgenol* 1992; 158: 101–5.

60 Konig H, Skalej M, Hontzsch D, Aicher K, Fortscher G E B. Kernspintomographie von knochen-knorpel-transplantaten im kniegelenk: transplantatmorphologie und Versuch einer quantitativen beurteilung der knorpelveranderunge. (Magnetic resonance tomography (MRT) and cartilage transplants on the knee). *Rontgenstr Nuklearmed* 1988; 148: 176–82.

61 Mink J H, Deutsch A L. Occult cartilage and bone injuries of the knee: detection, classification and assessment with MRI imaging. *Radiology* 1989; 170: 823–9.

62 Gylys-Morin V M, Hayek P C, Sartoris D J, Resnick D. Articular cartilage defects; detectability in cadaver knees with MRI. *Am J Roentgenol* 1987; 148: 1153–7.

63 Karoven R L, Negendank W G, Fraser S M, Mayes M D, An T, Fernandez-Madrid F. Correlation between magnetic resonance imaging and growth pathology. *Ann Rheum Dis* 1990; 49: 672–5.

64 Chandnani V P, Ho C, Chu P, Trudell D, Resnick D. Knee hyaline cartilage evaluated with MRI imaging—a cadaveric study involving multiple imaging sequences and intra-articular injection of gadolinium and saline solution. *Radiology* 1991; 178: 557–61.

65 Wojtys E, Wilson M, Buckwalter K, Braunstein E, Martel W. Magnetic resonance imaging of knee hyaline cartilage and intra-articular pathology. *Am J Sports Med* 1987; 15: 455–63.

66 Braunstein E M, Brandt K D, Albrecht M. MRI demonstration of hypertrophic articular cartilage repair in osteoarthritis. *Skel Radiol* 1990; 19: 335–9.

67 Sabiston C P, Adams M E, Li D K. Magnetic resonance imaging of osteoarthritis; correlation with gross pathology using an experimental model. *J Orthop Res* 1987; 5: 164–72.

68 Adam G, Nolte Ernsting C, Prescher A, *et al.* Experimental hyaline cartilage lesions: two-dimensional spin-echo versus three-dimensional gradient-echo imaging. *J Magn Reson Imaging* 1991; 1: 665–72.

69 Ho C, Cervilla V, Kjellin I, *et al.* Magnetic resonance imaging in assessing cartilages changes in experimental osteoarthrosis of the knee. *Invest Radiol* 1992; 27: 84–90.

70 Lehner K B, Rechl H P, Gmeinwieser J K, Heuck A F, Lukas H P, Kohl H P. Structure function and degeneration of bovine hyaline cartilage; assessment with MRI imaging in vitro. *Radiology* 1989; 170: 494–9.

71 Paul P K, O'Byrne E, Blancuzzi V, *et al.* Magnetic resonance imaging reflects cartilage proteoglycan degradation in the rabbit knee. *Skel Radiol* 1991; 20: 31–6.

72 Gahunia H K, Lemaire C, Cross A R, Babyn P, Kessler M J, Pritzker K P. Osteoarthritis in rhesus macaques: assessment of cartilage matrix quality by quantitative magnetic resonance imaging. *Agents Actions Suppl* 1993; 39: 255–9.

73 Watson P J, Hall L D, Carpenter T A, Tyler J A. A magnetic resonance imaging study of joint degeneration in the guiniea pig knee. *Agents Actions Suppl* 1993; 39: 261–5.